nature geoscience

Article

https://doi.org/10.1038/s41561-025-01868-0

Contrasting trends in very large hail events and related economic losses across the globe

Received: 10 March 2025

Accepted: 24 October 2025

Published online: 29 December 2025

Check for updates

Francesco Battaglioli[1,2] ✉, Mateusz Taszarek[3], Pieter Groenemeijer[1,4], Tomáš Púčik[4] & Anja Rädler[5]

Hailstorms producing hail larger than 5 cm cause the most severe damage to property and infrastructure, often leading to multibillion-dollar losses. Here we develop a global climatology of these very large hail events from 1950 to 2023 by combining statistical modelling with atmospheric reanalysis and examine trends in their frequency and related economic impacts. Northern Argentina emerges as the global hotspot of very large hail events, followed by Uruguay, Paraguay, southern Brazil, the US Great Plains and South Africa. Asia—and to a lesser extent, Europe and Australia—show substantially lower frequencies. Europe is seeing the sharpest rise in the frequency of very large hail events, driven by increasing low-level moisture and atmospheric instability. By contrast, the Southern Hemisphere—especially South America—is experiencing notable declines, linked to reduced mid-level humidity and instability. Hail-related losses have increased in the USA, Australia and Europe. In Europe, the rise is mainly due to more frequent very large hail events, whereas in the USA and Australia, increasing exposure and vulnerability are the primary drivers. These contrasting regional trends in hail frequency and related losses underscore the need for tailored risk management strategies that account for both climatic drivers and socio-economic vulnerabilities.

Hail is a primary contributor to insurance losses from severe convective storms (SCSs), with the USA accounting for 50–80% of insured SCS losses[1], resulting in annual damages between US$8 and US$14 billion (ref. 2). These losses are comparable to those caused by landfalling hurricanes[3]. Single hail events exceeding US$1 billion in economic loss have been recorded in the USA[4], Australia[5] and Europe[6], with northern Italy experiencing a record US$6 billion loss in 2023[1]. Small hail (<2 cm) can cause damage to agriculture[7], whereas direct damage to infrastructure, which contributes most to economic losses, increases sharply as hail becomes larger than 5 cm (ref. 8). Despite the higher socio-economic impacts of very large hail (VLH; ≥5 cm), research on global climatologies has focused on hail of smaller size[9,10]. These studies were also constrained by the coarse resolution of satellite and reanalysis datasets (ERA-Interim[11]) available at the time. The ERA5 reanalysis[12] offers higher spatial and temporal resolution, enhancing the representation of hail-favourable environmental conditions, although it does not simulate hail explicitly. To overcome this limitation, we apply a statistical model (additive regressive convective hazard model (AR-CHaMo)[13,14]) to generate a global climatology of VLH based on atmospheric variables such as instability, vertical wind shear and cloud base height. This model has proven effective in reconstructing the spatial distribution of VLH and the associated trends, even in regions lacking extensive ground-based observations[14]. Regional trend analyses have been conducted in the USA[15,16], Europe[13,17], Australia[18] and China[19]. However, not all of these studies have focused on VLH, and a comprehensive global analysis of these events remains absent. This work aims to address the existing knowledge gap by evaluating globally the long-term trends of VLH and the associated economic losses.

[1]European Severe Storms Laboratory e.V., Wessling, Germany. [2]ESSL Services GmbH, Wiener Neustadt, Austria. [3]Department of Meteorology and Climatology, Adam Mickiewicz University, Poznan, Poland. [4]European Severe Storms Laboratory—Science and Training, Wiener Neustadt, Austria. [5]Munich Re, Munich, Germany. ✉e-mail: francesco.battaglioli@essl.org

https://doi.org/10.1038/s41561-025-01868-0

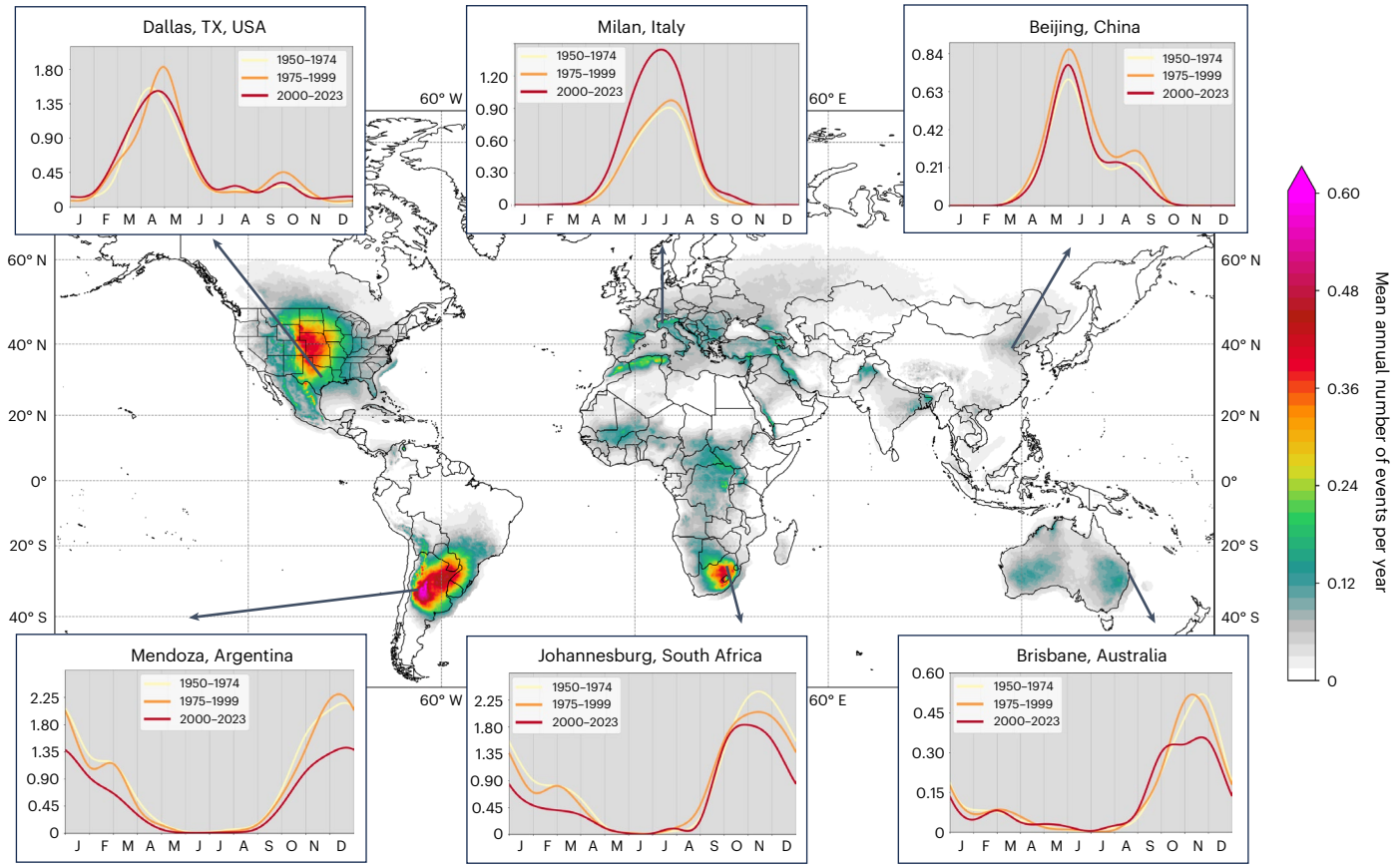

Fig. 1 | Mean annual number of VLH events between 1950 and 2023. The seasonal cycles for two 25-year periods (1950–1974 and 1975–1999) and one 24-year period (2000–2023) are shown for six locations: Dallas, TX, USA; Milan, Italy; Beijing, China; Mendoza, Argentina; Johannesburg, South Africa; and Brisbane, Australia. Maritime locations further than 100 km from the coast were excluded from the analysis. The bottom axes of the insets represent the months of the year.

The global climatology of very large hail

The AR-CHaMo models were applied to the ERA5 reanalysis, assigning a probability of VLH to every grid point (0.25° × 0.25° spatial resolution) for each 3-h period of the past 74 years, from 1950 to 2023. In total, more than 80 billion atmospheric profiles were used to construct the global climatology of VLH (Fig. 1).

The global maximum in VLH frequency is found in northern Argentina, where the mean annual number of VLH events is around 0.50, the equivalent of a VLH event every 2 years per grid box. The modelled spatial distribution aligns with previous studies[20], which report the highest frequency in the northern lee of the Argentina Andes. Here, VLH frequency peaks from November to February, although it has decreased in recent decades, particularly in December and January. Other areas of high VLH frequency include the tri-border region of Uruguay, Paraguay and Brazil. A smaller but non-zero VLH frequency extends also into the Central Andes region of Bolivia and southern Peru. Across South America, the necessary ingredients for hailstorms frequently overlap. The Andes foothills provide a focus for lift[21], while the South American low-level jet advects warm and moist air from the Amazon. This, combined with high deep vertical wind shear, provides an ideal environment for hailstorms[22].

In the USA, the Great Plains exhibit a high VLH frequency with a maximum located between Kansas, Nebraska and Colorado, aligning with radar-based climatologies[23,24]. The overlap of moisture from the Gulf of Mexico[25], elevated mixed layers generated over the high terrain of the southwest[26] and cyclonic activity in spring and early summer[27] provide a combination of high instability and wind shear, which makes the region a hail hotspot. A pronounced east–west gradient is observed across northern Texas, where VLH frequency peaks between March and June. The VLH seasonal cycle in Dallas corresponds with the dates of major hail events: 5 April 2003[28], 24 May 2011[4] and 11 June 2023[1]. In Canada, the frequency is lower, with the most affected areas being southern Saskatchewan and Alberta, in line with previous studies[29].

South Africa is another VLH hotspot, with a frequency exceeding 0.30 events per year in the northeast and along the Eastern Cape, where the Agulhas current provides moisture and the eastern Escarpment Mountains a focus for lift[30]. In Johannesburg, over the last two decades, the peak month of occurrence has shifted from November to October. VLH is also present in equatorial Africa, the western Sahel and northern Africa; however, a lack of ground-based reports and uncertainties in the accuracy of satellite-based estimates[31] complicate comparisons with observations in these regions.

VLH is less frequent in Europe, with the occurrence maximized in the lee of mountain ranges. High VLH frequency is found across northeastern Spain, southwestern France and northern Italy, which stands out as the European hotspot, in agreement with previous studies[17]. The seasonal cycle in Milan peaks in summer, although there is a tendency towards an earlier onset of VLH occurrence in spring. Other local maxima are observed in Switzerland, southern Germany and southeastern Austria, with VLH occurrence extending into southeast Europe. Further east, VLH frequency peaks locally in Turkey, Iran and the Arabian Peninsula, similar to ref. 9.

Asia experiences the lowest VLH activity, with northern Pakistan and Bangladesh having the highest frequency at around 0.12 events per year. VLH also peaks locally in northeastern China during spring and summer, whereas lower but non-zero VLH frequency is found over the Tibetan Plateau and southern China, consistent with ground-based report climatologies[32].

https://doi.org/10.1038/s41561-025-01868-0

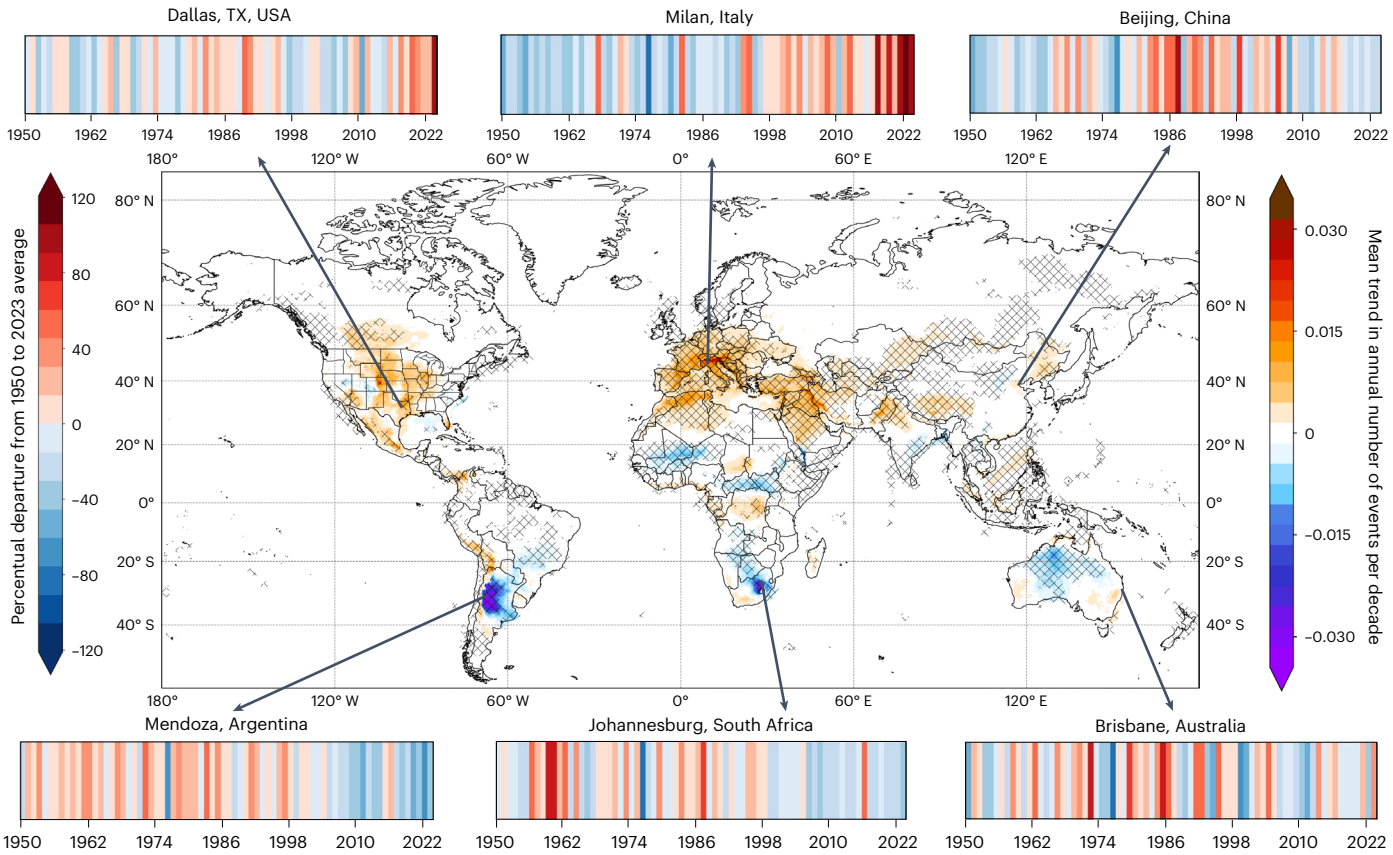

Fig. 2 | Mean trend in annual number of VLH events per decade between 1950 and 2023. The trends significant at a 95% level are hatched. Hail stripes (similar to ref. 14) displaying the yearly percentage departure from the long-term average are plotted for the same locations as in Fig. 1.

In Australia, VLH is most frequent in the east, as shown by ref. 33. A second maximum is present in the southwest interior, similar to ref. 13, though reports in this area are rare owing to low population density, and the limited radar coverage prevents the direct verification of these findings.

The global climate trends of very large hail

Trends in VLH frequency (1950–2023) are not globally homogeneous but exhibit a strong zonal dependence: positive and significant trends are almost exclusively present in the Northern Hemisphere, whereas negative trends are limited to the Southern Hemisphere (Fig. 2).

Europe is the only continent to exhibit a widespread and statistically significant increase in VLH frequency, extending into northern Africa and the Middle East. These findings align with pan-European[8,13,34] and regional analyses from single countries (for example, Switzerland[35]). Northern Italy shows the largest global increase in VLH frequency (up to +0.03 events per decade). In Milan, VLH frequency has consistently exceeded the 1950–2023 average over the last two decades, with 2021–2023 marking the most active years. This period corresponds with a record number of hail reports in Italy, including a 19-cm hailstone in July 2023[36].

North America displays positive VLH trends, particularly in southern Canada, where southern Alberta has the largest increase (+0.01 events per decade). An increase of similar magnitude is also seen in the mountainous regions of Mexico. The trends are mostly not significant in the USA except for very localized increases in the Great Plains. Compared with previous work focusing on hail-prone environments[15], the increase is more localized, although a tendency for very large hailstones to become more frequent has been shown in recent studies[16]. In Dallas, VLH frequency has increased by 43.4% since the 1950s, and 2023 was the most active year, with a +105% departure from the 1950–2023 average. This aligns with the record losses reported across Texas in the year 2023[37].

In northern Argentina, VLH frequency has decreased the most. The decrease is steady in Mendoza, where every year since 2006, except for 2015 and 2016, has experienced below-average VLH frequency (mean of −29.8%). This decrease is supported by a reduction in hail reports[38]. Localized positive trends are found in Bolivia and Peru.

South Africa has the second-largest VLH decrease, especially in the northeast, where the decadal trend reaches −0.02 events per decade. This trend is also supported by a general reduction in severe thunderstorm environments[39]. Negative trends are observed locally in Equatorial Africa, although they remain unverified owing to a lack of direct observations. By contrast, northern Africa shows a positive VLH frequency trend comparable in magnitude to that of mainland Europe, as noted by ref. 13.

In Asia, VLH frequency trends are generally small or non-existent. However, positive and significant trends are present across Pakistan, the Tibetan Plateau and northeastern China. In Beijing, above-average VLH activity occurred in the 1980s, followed by a decreasing trend in hail days from 1980 to 2005[19]. Negative and significant trends in the region are limited to the eastern coast of India.

In Australia, the trends are largely negative in the continental areas of the north with low VLH frequency (Fig. 1), whereas coastal regions show no significant trend. In Brisbane, a strong year-to-year variability is present, and trends are not significant, as also shown by ref. 13.

In conclusion, it is important to note that trends in VLH frequency are sensitive to the period considered. Trends between 1979 and 2023 exhibit stronger negative values in the Southern Hemisphere, regional differences in the USA and a broadly similar pattern across Europe when compared with the 1950–2023 period (Supplementary Fig. 1).

https://doi.org/10.1038/s41561-025-01868-0

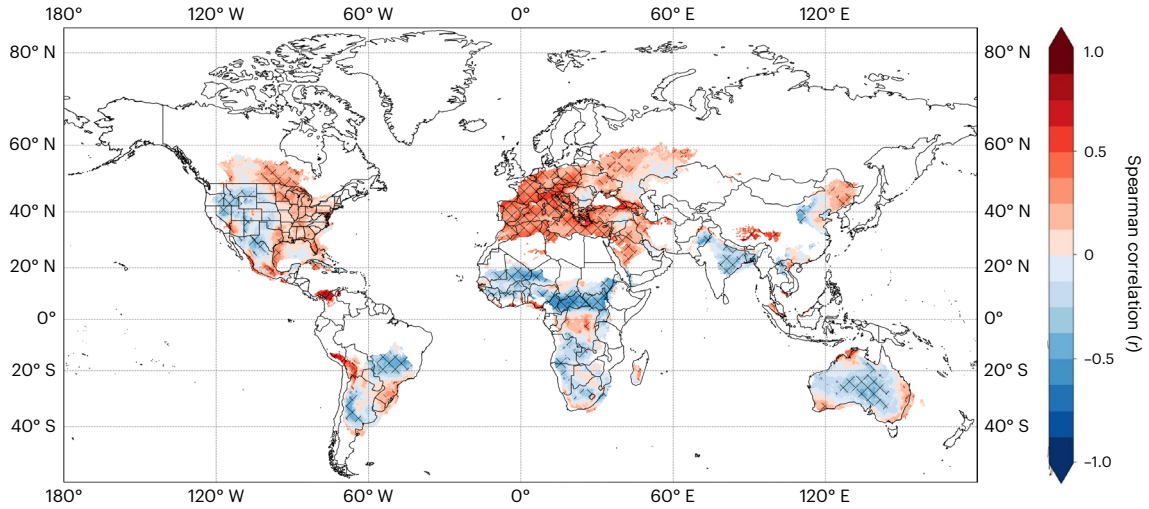

Fig. 3 | Grid-based Spearman rank-order correlation (*r*) between yearly VLH frequency and 2-m temperature yearly mean for the period 1950–2023. The areas with a correlation significant at a 95% level (*P* value <0.05) are hatched. To display only VLH-prone regions, values over areas with a low mean annual VLH frequency (<0.09 events per year) are not shown.

Hail trends attribution and relationship with global warming

The relationship between temperature change and VLH trends is not uniform globally (Fig. 3).

Europe is the only region where an increase in 2-m temperature significantly correlates with higher VLH frequency, especially in southern Europe ($r \approx 0.7$), the Mediterranean, Turkey and the Middle East. This positive correlation reflects an increase in instability and thunderstorm intensity[14,39]. In the USA, the correlation is weaker and spatially heterogeneous, with positive values in the east and negative ones in the west, where drying in the mid-levels reduces storm potential[26,39].

In South America, a bimodal pattern appears along the lee of the Andes, with positive correlations ($r \approx 0.7$) in Peru and Bolivia but negative ones in Argentina. Similar patterns occur in southern and central Brazil; however, correlations remain small ($-0.3 < r < +0.3$), suggesting that other factors might better explain VLH frequency trends. In Africa, correlations are generally small and nonsignificant, except in the Sahel region, where $r \approx -0.5$. This area coincides with a marked decrease in convective precipitation[39]. Correlations vary by region but remain small in Australia, ranging from −0.3 inland to +0.3 on the coast. The correlation mirrors low-level moisture patterns in the east, with inland drying and increasing coastal moisture (Supplementary Figs. 2 and 3), which corresponds to increasing instability[18] and storm potential. In conclusion, the decrease in VLH frequency observed across most hail-prone regions of the Southern Hemisphere (Fig. 2) seems to be attributable to a combination of a decrease in low-level moisture, instability in the cold part of the storm and locally wind shear (Supplementary Figs. 2 and 3).

Although temperature as a stand-alone parameter does not represent an ingredient for storm or hail formation, changes in its values can correlate with changes in storm ingredients, influencing VLH frequency.

Northern Italy and northwestern Argentina: quantitative trend attribution

Observing that upward 2-m temperature trends coincide with both increasing and decreasing trends in VLH frequency prompts us to investigate the drivers of these changes. We focus on two regions with the most pronounced and opposite trends, northern Italy and northwestern Argentina, and analyse the contributions of the various predictor parameters of the VLH model (Supplementary Table 1) to the trends depicted in Fig. 2. A detailed breakdown of parameter contributions for both northern Italy and northwestern Argentina is provided in Supplementary Table 2.

In northern Italy, the sum of all predictors' contributions is +72.8%. Although thunderstorms have become slightly less frequent (−6.3%), their severity has substantially increased. More specifically, the probability that a storm will be capable of producing VLH has risen by 79.1%. This increase is mainly due to the rising atmospheric instability in the cold part of the storm (Supplementary Fig. 3), which results from enhanced latent heat release and higher water vapour content. This aligns with previous findings[13,40], suggesting that increased instability leads to stronger storms in the mid-latitudes.

In northwestern Argentina, the sum of all predictors' contributions is −24.5%. Thunderstorms have both become less frequent (−15.9%) and less prone to producing VLH (−8.6%). The reduction in thunderstorm likelihood is consistent with patterns of increasing drought[41] and is primarily attributed to declining low and mid-level moisture and instability (Supplementary Figs. 2 and 3).

Trends in insured losses across Europe, the USA and Australia

Understanding the relationship between changes in VLH frequency and hail losses is crucial, given the significant economic impacts of hail[8]. We analysed trends in hail loss events (Methods) in regions with high insurance penetration: Germany, Austria, Benelux countries (Europe), the eastern two thirds of the USA and populated coastal regions of Australia (Supplementary Fig. 4). To compare long-term trends in hail loss events with VLH frequencies, we aggregated VLH probabilities over the selected domains from 1993 to 2023 (Fig. 4).

Over the past 30 years, hail loss events have increased in Europe (Germany, Austria, Benelux), the USA and Australia, driven by a combination of social, economic and environmental factors[42]. The modelled VLH frequency generally reproduces yearly variations in annual loss events well, especially in Europe between 1998 and 2007. The correlation between the trends in VLH frequency and those in hail loss events suggests that increasing VLH occurrence strongly contributes to the rise in hail loss events in Europe. Several differences exist in the two time series for the most recent years, meaning that trends in a longer time series may diverge. By contrast, the USA and Australia display different patterns. While VLH frequency increased only slightly in the USA and decreased in Australia, hail loss events continued to rise in both regions. This discrepancy suggests that socio-economic factors, such as changes in exposure and vulnerability, are more important drivers of the increase in hail loss events than meteorological factors. These findings are consistent with previous research on tornadoes in

https://doi.org/10.1038/s41561-025-01868-0

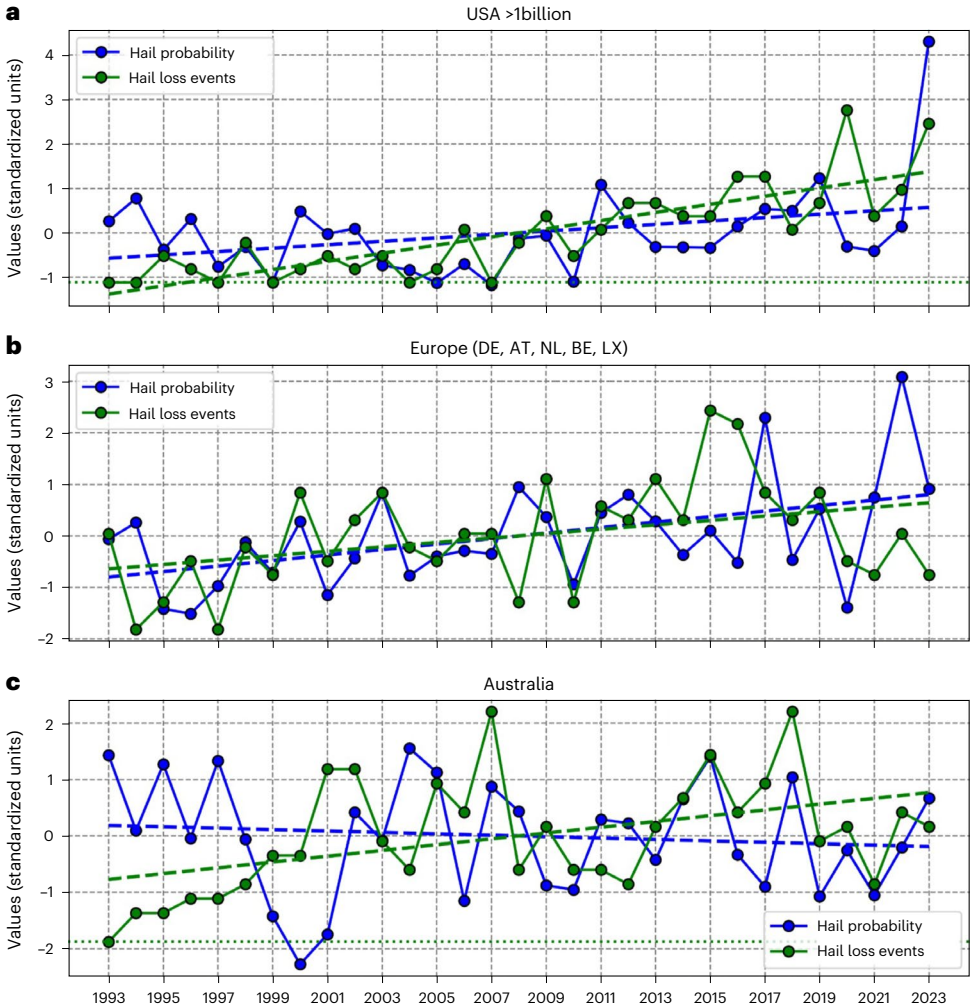

Fig. 4 | Comparison between changes in VLH frequency and hail loss events. **a**–**c**, The time series of the standardized mean annual sum of VLH probabilities (blue line) and hail loss events (green line) for the eastern two thirds of the USA (**a**), Germany (DE), Austria (AT) and the Benelux (NL, BE, LX) countries (Europe) (**b**) and coastal Australia (**c**). Hail loss events are defined as the entries recorded in Munich RE's NatCatSERVICE Database, for which the primary cause of loss is due to hail. The linear trends are shown as dashed lines. The dotted green line in the USA and Australia graphs corresponds to zero hail loss events. This figure was created by co-author A.R., who was granted permission to publish by Munich RE.

the USA[43,44]. In conclusion, it is important to note that across sparsely populated regions, such as Australia, losses only occur where the exposure is concentrated. For this reason, the comparison between trends in VLH frequency and those in hail loss events may differ from Fig. 4 when single metropolitan regions are considered (Supplementary Fig. 5).

Global implications of very large hail trends

We reconstructed the global occurrence of VLH over a period of 74 years (1950–2023) using an additive logistic regression model (AR-CHaMo) trained with lightning observations, hail reports and atmospheric predictors from the ERA5 reanalysis across Europe, the USA and Australia. VLH is most frequent across northern Argentina and the border regions of Uruguay, Paraguay and Brazil. High VLH frequency is also modelled in the US Great Plains and parts of South Africa. While VLH is less frequent in other regions (Europe, Africa, Oceania and Asia), the reconstruction aligns with regional climatologies in both the simulated spatial distribution and the seasonal patterns. In addition, the recent extreme hail activity in the USA and Europe is well represented by the model, with 2023 standing out as the year with the highest VLH frequency.

Although no universally valid relationship between VLH trends and global warming has been identified, several significant regional correlations exist. In Europe, VLH frequency has increased the most, correlating with rising temperatures. Trends are especially pronounced in northern Italy, driven by an increase in low-level moisture and instability in the cold part of storms. Other regions with positive significant trends include the Middle East, southern Canada, parts of Mexico and localized areas in the USA. Increasing temperatures do not always correlate with an increase in VLH frequency: in the western USA and continental Australia, drying has reduced the storm potential. Negative trends in VLH frequency are observed mainly in the Southern Hemisphere, with the strongest declines in South Africa and northern Argentina, where they are primarily driven by a decrease in mid-level humidity and instability.

Finally, we examined the relationship between changes in VLH frequency and those in hail loss events. Hail loss events have increased in parts of Europe, the USA and Australia. In Europe, rising VLH occurrence contributes to the increase in hail losses, along with growing exposure and vulnerability. In the USA and Australia, changes in meteorological conditions do not correlate with the increase in hail loss events; instead, exposure and vulnerability drive the increase. To confirm this hypothesis, future studies should dive deeper into the topic of loss normalization or investigate trends in exposure and vulnerability.

Several limitations must be considered when interpreting these results. The VLH model, trained on three mid-latitude regions, was

applied globally; therefore, results should be interpreted with caution in areas where regional climatologies do not enable verification or known biases in ERA5 are present (for example, the tropics[45]). Future research should incorporate newly available databases from regions such as South America, Canada and China to better capture hail environments on a global scale. Another area of future research concerns the use of reanalysis data at a higher resolution to explicitly simulate storm development, which was not possible in ERA5.

Despite the limitations, this study provides a comprehensive analysis of the climatological occurrence of VLH, the associated long-term trends in the context of a warming climate and the relationship with losses on a global scale.

Online content

Any methods, additional references, Nature Portfolio reporting summaries, source data, extended data, supplementary information, acknowledgements, peer review information; details of author contributions and competing interests; and statements of data and code availability are available at https://doi.org/10.1038/s41561-025-01868-0.

References

1. Bowen, S. Kerschner, B. & Ng, J. Z. *Natural Catastrophe and Climate Report: 2023* (Gallagher Re, accessed 3 Dec 2024); https://www.ajg.com/gallagherre/-/media/files/gallagher/gallagherre/news-and-insights/2024/january/natural-catastrophe-and-climate-report-2023.pdf
2. Podlaha, A., Bowen, S. & Lörinc, M. *Weather, Climate and Catastrophe Insight: 2019 Annual Report* (Aon, 2020); http://thoughtleadership.aon.com/Documents/20200122-if-natcat2020.pdf
3. Gunturi, P., & Tippett, M. K. *Managing Severe Thunderstorm Risk: Impact of ENSO on U.S. Tornado and Hail Frequencies* (Willis Re, 2017).
4. Brown, T. M., Pogorzelski, W. H. & Giammanco, I. M. Evaluating hail damage using property insurance claims data. *Weather Clim. Soc.* **7**, 197–210 (2015).
5. Schuster, S., Blong, R., Leigh, R. & McAneney, K. Characteristics of the 14 April 1999 Sydney hailstorm based on ground observations, weather radar, insurance data and emergency calls. *Nat. Hazards Earth Syst. Sci.* **5**, 613–620 (2005).
6. Kunz, M. et al. The severe hailstorm in southwest Germany on 28 July 2013: characteristics, impacts and meteorological conditions. *Quart. J. Roy. Meteorol. Soc.* **144**, 231–250 (2018).
7. Rana, V. S. et al. Management of hailstorms under a changing climate in agriculture: a review. *Environ. Chem. Lett.* **20**, 3971–3991 (2022).
8. Púčik, T. et al. Large hail incidence and its economic and societal impacts across Europe. *Mon. Weather Rev.* **147**, 3901–3916 (2019).
9. Prein, A. & Holland, G. Global estimates of damaging hail hazard. *Weather Clim. Extrem.* **22**, 10–23 (2018).
10. Bang, S. & Cecil, D. Constructing a multifrequency passive microwave hail retrieval and climatology in the GPM domain. *J. Appl. Meteorol. Climatol.* **58**, 1889–1904 (2019).
11. Dee, D. et al. The ERA-INTERIM reanalysis: configuration and performance of the data assimilation system. *Quart. J. Roy. Meteorol. Soc.* **137**, 553–597 (2011).
12. Hersbach, H. et al. The ERA5 global reanalysis. *Quart. J. Roy. Meteorol. Soc.* **146**, 1999–2049 (2020).
13. Rädler, A., Groenemeijer, P., Faust, E. & Sausen, R. Detecting severe weather trends using an additive regressive convective hazard model (AR-CHaMo). *J. Appl. Meteorol. Climatol.* **57**, 569–587 (2018).
14. Battaglioli, F. et al. Modeled multidecadal trends of lightning and (very) large hail in Europe and North America (1950–2021). *J. Appl. Meteorol. Climatol.* **62**, 1627–1653 (2023a).
15. Tang, B., Gensini, V. & Homeyer, C. Trends in United States large hail environments and observations. *NPJ Clim. Atmos. Sci.* **2**, 45 (2019).
16. Gensini, V. A. et al. Hail size dichotomy in a warming climate. *NPJ Clim. Atmos. Sci.* **7**, 185 (2024).
17. Punge, H., Bedka, K., Kunz, M. & Reinbold, A. Hail frequency estimation across Europe based on a combination of overshooting top detections and the ERA-INTERIM reanalysis. *Atmos. Res.* **198**, 34–43 (2017).
18. Raupach, T. H., Soderholm, J. S., Warren, R. A. & Sherwood, S. C. Changes in hail hazard across Australia: 1979–2021. *NPJ Climate Atmos. Sci.* **6**, 143 (2023).
19. Zhang, C., Zhang, Q. & Wang, Y. Climatology of hail in China: 1961–2005. *J. Appl. Meteorol. Climatol.* **47**, 795–804 (2008).
20. Mezher, R. N., Doyle, M. & Barros, V. Climatology of hail in Argentina. *Atmos. Res.* **114–115**, 70–82 (2012).
21. Rasmussen, K. L. & Houze, R. A. Orogenic convection in subtropical South America as seen by the TRMM satellite. *Mon. Weather Rev.* **139**, 2399–2420 (2011).
22. Bechis, H. et al. A case study of a severe hailstorm in Mendoza, Argentina, during the RELAMPAGO-CACTI field campaign. *Atmos. Res* **271**, 106127 (2022).
23. Murillo, E., Homeyer, C. & Allen, J. A 23-year severe hail climatology using GridRad MESH observations. *Mon. Weather Rev.* **149**, 945–958 (2023).
24. Wendt, N. & Jirak, I. An hourly climatology of operational MRMS MESH-diagnosed severe and significant hail with comparisons to storm data hail reports. *Weather Forecast.* **36**, 645–659 (2021).
25. Molina, M. J., Timmer, R. P. & Allen, J. T. Importance of the Gulf of Mexico as climate driver for U.S. severe thunderstorm activity. *Geophys. Res. Lett.* **43**, 12,295–12,304 (2016).
26. Andrews, M. S. et al. Climatology of the elevated mixed layer over the contiguous United States and Northern Mexico using ERA5: 1979–2021. *J. Clim.* **37**, 1833–1851 (2024).
27. Li, F., D. R. Chavas, Need, K. A., Rosenbloom, N. & Dawson, D. T. The role of elevated terrain and the Gulf of Mexico in the production of severe local storm environments over North America. *J. Clim.* **34**, 7799–7819 (2021).
28. Marshall, T. P., Herzog, R. F., Mitchell, D. E., Morrison, S. J. & Rae, S. The Dallas–Ft. Worth, TX Hailstorm: 5 April 2003. In *22nd Conference on Severe Local Storms* 9.1 (2004); https://ams.confex.com/ams/11aram22sls/techprogram/paper_81089.htm
29. Brunet, D. & Brimelow, J. A hail climatology for canada using a lightning proxy. *J. Appl. Meteorol. Climatol.* **63**, 1227–1240 (2024).
30. Blamey, R. C., Middleton, C., Lennard, C. & Reason, C. J. C. A climatology of potential severe convective environments across South Africa. *Clim. Dyn.* **49**, 2161–2178 (2017).
31. Ferraro, R., Beauchamp, J., Cecil, D. & Heymsfield, G. A prototype hail detection algorithm and hail climatology developed with the Advanced Microwave Sounding Unit (AMSU). *Atmos. Res.* **163**, 24–35 (2015).
32. Ni, X., Muehlbauer, A., Allen, J. T., Zhang, Q. & Fan, J. A climatology and extreme value analysis of large hail in China. *Mon. Weather Rev.* **148**, 1431–1447 (2020).
33. Brook, J. P., Soderholm, J. S., Protat, A., McGowan, H. & Warren, R. A. A radar-based hail climatology of Australia. *Mon. Weather Rev.* **152**, 607–628 (2024).
34. Taszarek, M., Allen, J., Brooks, H., Pilguj, N. & Czernecki, B. Differing trends in United States and European severe thunderstorm environments in a warming climate. *Bull. Am. Meteorol. Soc.* **102**, 296–322 (2021a).
35. Wilhelm, L., Schwierz, C., Schröer, K., Taszarek, M. & Martius, O. Reconstructing hail days in Switzerland with statistical models (1959–2022). *Nat. Hazards Earth Syst. Sci.* **24**, 3869–3894 (2024).
36. European Severe Weather Database. *ESWD* https://eswd.eu (accessed 6 April 2024).

37. Natural disasters of 2023. *Munich RE* https://www.munichre.com/en/company/media-relations/media-information-and-corporate-news/media-information/2024/natural-disaster-figures-2023.html (2024).
38. Beal, A. et al. Climatology of hail in the triple border Paraná, Santa Catarina (Brazil) and Argentina. *Atmos. Res.* **234**, 104747 (2020).
39. Taszarek, M., Allen, J. T., Marchio, M. & Brooks, H. E. Global climatology and trends in convective environments from ERA5 and rawinsonde data. *NPJ Clim. Atmos. Sci.* https://doi.org/10.1038/s41612-021-00190-x (2021b).
40. Pilguj, N., Taszarek, M., Kryza, M. & Brooks, H. Reconstruction of violent tornado environments in europe: high-resolution dynamical downscaling of ERA5. *Geophys. Res. Lett.* https://doi.org/10.1029/2022GL098242 (2022).
41. Feron, S. et al. South America is becoming warmer, drier, and more flammable. *Commun. Earth Environ.* **5**, 501 (2024).
42. Kron, W., Steuer, M., Löw, P. & Wirtz, A. How to deal properly with a natural catastrophe database—analysis of flood losses. *Nat. Hazards Earth Syst. Sci.* **12**, 535–550 (2012).
43. Strader, S. M., Ashley, W. S., Pingel, T. J. & Krmenec, A. J. Projected 21st century changes in tornado exposure, risk, and disaster potential. *Climatic Change* **141**, 301–313 (2017).
44. Bouwer, L. M. in *Loss and Damage from Climate Change* 63–82 (Springer, 2019); https://doi.org/10.1007/978-3-319-72026-5_3
45. Taszarek, M. et al. Comparison of convective parameters derived from ERA5 and MERRA2 with rawinsonde data over Europe and North America. *J. Clim.* **34**, 1–55 (2021c).

Methods

AR-CHaMo models

AR-CHaMo[13,14] is a logistic regression model that yields the probability of VLH as a function of environmental predictors from the atmospheric reanalysis (listed in Supplementary Table 1) that were calculated using the ThundeR rawinsonde package[46]. AR-CHaMo calculates this probability by combining the likelihood of a thunderstorm ($P_{\text{lightning}}$) and the conditional probability of VLH given a thunderstorm ($P_{\text{VLH/lightning}}$). $P_{\text{lightning}}$ was trained simultaneously using lightning observations (over five million) from the Arrival Time Difference Network[47] across Europe (34.5°–63.5° N, 9.0° W–46.0° E), the National Lightning Detection Data (NLDN[48]) from the USA (29.0°–41.5° N, 109.0°–79.0° W) and the Global Position and Tracking Systems (GPATS[49]) from Australia (10.5°–40.0° S, 119.0°–153.5° E). $P_{\text{VLH/lightning}}$ was trained simultaneously using hail reports (over 4,500) from the European Severe Weather Database (45.0°–54.0° N, 5.0°–22.0° E), the Storm Prediction Centre Storm Archive (30.5°–41.5° N, 105.0°–82.0° W) and the Australian Bureau of Meteorology (22.5°–37.5° S, 149.5°–153.5° E). $P_{\text{lightning}}$ was improved by using a grid-based ratio between lightning observations from the Earth Networks Global Lightning Detection Network[50] and modelled lightning occurrence, improving the lightning distribution, especially across (sub)tropical regions where AR-CHaMo was not trained. The mean annual expected number of VLH events was calculated as the sum of all 3-h probabilities in a year multiplied by three. To do so, we assumed 3-h probabilities to be independent of each other, although this may not strictly be the case.

Insurance loss data

The data on hail losses were obtained from the NatCatSERVICE database of Munich RE[42]. Within the database, each loss entry includes its type, location, date, loss and description. Using the description, we filtered only for events where the loss was at least partly caused by hail, ensuring that events caused exclusively by other convective hazards were not taken into consideration. Single events often covered multiple days, meaning that those entries included multiple SCS events. In these cases, the loss location coordinates indicate the loss centre. To account for inflation, urban growth and regional wealth differences, the estimated overall losses were normalized to the 2019 levels of destructible wealth. For 2020 to 2023, we used the inflation-adjusted values of the losses. Normalization was done by considering the Gross Domestic Product discretized on a 1° × 1° grid.

The accuracy of the loss estimates depends on the insurance penetration in a given country for a specific hazard[42]. In Europe, we selected Germany, the Benelux countries and Austria. Australia was also considered, given the fact that hail causes substantial losses[5], similar to the USA[37]. For the USA, we applied a threshold of US$1 billion to capture the most impactful events and to limit the chances that 'minor' events were missed in the early times[42].

Data availability

ERA5 hourly data on single levels can be obtained from the Copernicus Climate Data Store at https://cds.climate.copernicus.eu/datasets/reanalysis-era5-single-levels?tab=overview. Convective parameters from ERA5 data are calculated using the open-source ThundeR package that is publicly available at http://www.rawinsonde.com/thunder_app/. US hail reports are available from the Storm Prediction Centre Storm Archive (https://www.spc.noaa.gov/exper/archive/events/), Australian hail reports are available from the Bureau of Meteorology (http://www.bom.gov.au/australia/stormarchive/) and European ones can be obtained from the European Severe Weather Database (https://eswd.eu/). ENGLN global lightning observations are publicly available at http://thunderhours.earthnetworks.com, whereas regional ones were obtained for this study and are property of the Met Office (ATDnet), Vaisala (NLDN) and the Bureau of Meteorology (GPATS). The NatCatSERVICE dataset is property of Munich RE and was made available exclusively for this study. However, all data necessary to reproduce all figures and findings—including but not limited to the global climatologies and trends—are available via Zenodo at https://doi.org/10.5281/zenodo.17064885 (ref. 51). Source data are provided with this paper.

Code availability

All figures were generated with the open-source software Python. The codes are available as a Jupyter Notebook alongside the data to reproduce the figures via Zenodo at https://doi.org/10.5281/zenodo.17064885 (ref. 51).

References

46. Taszarek, M., B. Czernecki, & Szuster, P. thundeR—a rawinsonde package for processing convective parameters and visualizing atmospheric profiles. In *11th European Conference on Severe Storms* https://doi.org/10.5194/ecss2023-28
47. Enno, S., Sugier, J., Alber, R. & Seltzer, M. Lightning flash density in Europe based on 10 years of ATDnet data. *Atmos. Res.* **235**, 104769 (2020).
48. Koehler, T. Cloud-to-ground lightning flash density and thunderstorm day distributions over the contiguous United States derived from NLDN measurements: 1993– 2018. *Mon. Weather Rev.* **148**, 313–332 (2020).
49. Dowdy, A. J. & Kuleshov, Y. Climatology of lightning activity in Australia: spatial and seasonal variability. *Aust. Meteorol. Oceanogr. J.* **64**, 103–108 (2014).
50. DiGangi, E. A., Stock, M. & Lapierre, J. Thunder hours: how old methods offer new insights into thunderstorm climatology. *Bull. Am. Meteorol. Soc.* **103**, E548–E569 (2022).
51. Battaglioli, F. NGS_2025_03_00751. *Zenodo* https://doi.org/10.5281/zenodo.17064885 (2025).

Acknowledgements

M.T.'s contribution was funded by a grant from the Polish National Science Centre (grant no. 2020/39/D/ST10/00768). The ERA5 reanalysis computations were performed in the Poznan Supercomputing and Networking Centre (grant no. 648). A.R.'s contribution was supported by Munich RE.

Author contributions

F.B. conceived the idea and designed this study. F.B. performed the analysis, wrote the manuscript and produced all figures apart from Fig. 4 (A.R.). M.T. calculated environmental predictors from the ERA5 reanalysis using the ThundeR package and contributed to the interpretation of the results. P.G. and T.P. greatly contributed to the scientific analysis of the results together with A.R., who jointly wrote the 'Trends in insured losses across Europe, the USA and Australia' section with F.B.

Competing interests

The authors declare no competing interests.

Additional information

Supplementary information The online version contains supplementary material available at https://doi.org/10.1038/s41561-025-01868-0.

Correspondence and requests for materials should be addressed to Francesco Battaglioli.

Peer review information *Nature Geoscience* thanks Mathis Tonn and the other, anonymous, reviewer(s) for their contribution to the peer review of this work. Primary Handling Editors: Stefan Lachowycz, Aliénor Lavergne, Tom Richardson, in collaboration with the *Nature Geoscience* team.